

# MHD Stagnation point flow with Dufour Diffusivity and Impermeability of the surface.

Abubakar Assidiq Hussaini<sup>\*1</sup>, Adamu Abdulkadir Tata<sup>2</sup>,  
Ja'afar Aliyu<sup>3</sup>

<sup>\*1</sup> Department of Mathematical Sciences, Abubakar Tafawa Balewa University, Bauchi.  
<sup>2,3</sup> Department of Mathematics and Statistics, Federal Polytechnic Bauchi.

Date of Submission: 01-09-2022

Date of Acceptance: 10-09-2022

## ABSTRACT

The intent of current research is to identify and explore the footprint of magnetohydrodynamic stagnation point flow across a convective surface in which impermeability of the surface, Dufour diffusivity, heat generation/absorption, magnetic field intensity, Biot number, non-linear radiative heat, among other parameters are accounted. Convection and diffusive boundary conditions are deemed. The governing flow equations for the flow fields are converted into non-dimensional form by using appropriate similarity variables. These ODEs are solved by fourth order Runge–Kutta and Shooting method. The outcomes are bestowed with plots and table for the influence of diverse flow variables on the flow fields. It was observed that temperature depreciates and concentration appreciate with the upsurge in Sorret number, whereas a negative impact is perceived with Dufour number. A decrement in Nusselt number and an enhancement in Sherwood number are observed for the intensification of non-linear radiative parameter.

**Keywords:** Stagnation Point, Magnetohydrodynamic, Stretching surface, Impermeability, Dufour diffusivity.

## I. MATHEMATICAL ANALYSIS

We investigated continuous 2 dimensional boundary layer flow of a nanofluid in the presence of a Dufour diffusivity alongside impermeability of the surface via solar radiation, as illustrated in Figure 1 below. magnetic field of homogeneous strength as well as heat generation/ absorption are also taken into consideration.

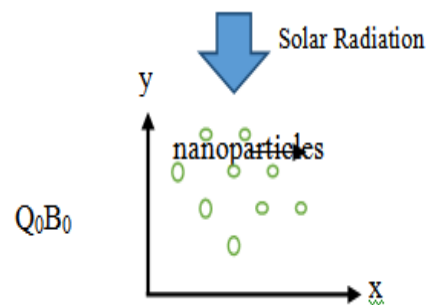


Fig. 1 Coordinate system of physical model

The orientations are such that the sheet is stretched along the x-axis and perpendicular to the y-axis. The velocity at the sheet surface (wall) is kept constant over the distance x, and x is the sheet coordinate, and the sheet velocity is zero. The transverse magnetic field is exposed to flow normal to the fluid flow direction along the positive y. The external electrical field is Assumed to be 0, also the electrical field induced by charge polarization is insignificant. After which the mass transfer analysis is carried out, taking into account the impacts of Dufour Diffusivity, impermeability, chemical reaction, heat generation/absorption as well as the other relevant characteristics. The sheet surface temperature  $T_w$  corresponds to the quiescent fluid temperature  $T_f$  during the convective heating process.  $T$  is the temperature of the surrounding fluid.  $C$  stands for nanoparticle concentration,  $C_w$  for nanoparticle concentration at the wall, and  $C_\infty$  for ambient concentration.

Based on the conventional boundary layer assumptions, these are the governing equations for the conservation of Mass, Momentum, Temperature, and Nanoparticle Concentration in the presence of Dufour Diffusivity and

Impermeability of the surface as in Ghasemi et al. (2021):

$$\frac{\partial u}{\partial y} + \frac{\partial u}{\partial y} = 0 \quad \dots \quad (1).$$

$$u \frac{\partial u}{\partial x} + v \frac{\partial u}{\partial y} = U_\infty \frac{du_\infty}{dx} + v_f \frac{\partial^2 u}{\partial x^2} - \frac{\sigma_e B_0^2}{\rho_f} (u - u_\infty) + \frac{\mu_e}{k} u \quad \dots \quad (2).$$

$$u \frac{\partial T}{\partial x} + v \frac{\partial T}{\partial y} = \alpha \frac{\partial^2 T}{\partial y^2} + \frac{v_f}{C_f} \left( \frac{\partial u}{\partial y} \right)^2 - \frac{1}{(\rho C)_f} \left( \frac{\partial q_r}{\partial y} \right) + \frac{\sigma_e B_0^2}{(\rho C)_f} (u_\infty - u)^2 + \tau D_B \left[ \frac{\partial T}{\partial y} \frac{\partial C}{\partial y} + \frac{D_T}{T_\infty} \left( \frac{\partial T}{\partial y} \right)^2 \right] \dots (3).$$

$$u \frac{\partial C}{\partial y} + v \frac{\partial C}{\partial y} = D_B \frac{\partial^2 C}{\partial y^2} + \frac{D_T}{T_\infty} \frac{\partial^2 T}{\partial y^2} + D_{TC} \frac{\partial^2 T}{\partial y^2} \quad \dots \quad (4).$$

where  $v_f$  denotes kinematic viscosity,  $\sigma_e$  denotes fluid electrical conductivity,  $B_0$  denotes a uniform magnetic field along the y-axis,  $u$  and  $v$  denote velocity components in the x and y axes respectively,  $\tau = \frac{(\rho C)_p}{(\rho C)_f}$ , stands for the ratio of

the effective heat capacity of nanoparticles to the heat capacity of the base fluid, where  $q_r$  denotes the quantity of radiative heat flux. By the radiative heat flux can be calculated using the Rosseland approximation for thermal radiation and applied to optically thick medium. as well as [Raptis (1998), Brewster (1972) and Sparrow and Sparrow (1978)].

The Stefan-Boltzman constant and the mean absorption coefficient are represented by  $\sigma^*$  and  $k^*$ , respectively. The nonlinear Rosseland approximation is employed for radiative heat flux modeling based on earlier works [Mushtaq et al. (2014), Ghasemi et al. (2016), Ghasemi et al. (2021)]. As a result, the relevant convective heat transfer boundary conditions can be written as

$$at \ y = 0: -k \frac{\partial T}{\partial y} = h(T - T_f), \ C = C_w$$

$$at \ y \rightarrow \infty: T \rightarrow T_\infty, \ C \rightarrow C_\infty \quad \dots \quad (6)$$

Together with the following dimensionless variables as in Ghasemi et al. (2021)

$$\eta = \sqrt{\frac{a}{v_f}} y, \ u = axf'(\eta), \ v = -\sqrt{av_f} f(\eta) \quad \dots \quad (7)$$

The first term on the right hand side for Eq. (2) will be transferred to

$$\alpha \frac{\partial}{\partial y} \left[ \frac{\partial T}{\partial y} (1 + R_d (\theta_w - 1) \theta^3) \right], \text{ where } R_d = 16\sigma^* T_\infty^3 / 3kk^*$$

by defining the non-dimensional temperature profile as  $\theta(\eta) = T - T_\infty / T_f$  with

$$T = T_\infty (1 + (\theta_w - 1) \theta) \text{ and } R_d = 0 \text{ is the scenario when there is no thermal radiation impact. The last statement can also be simplified to } \frac{\alpha(T_f - T_\infty)}{\text{Pr}} \left[ (1 + R_d (1 + (\theta_w - 1) \theta^3) \theta') \right], \text{ Pr}$$

denotes the Prandtl number which is given by  $\text{Pr} = v_f / \alpha$

By introducing the boundary conditions eq. (6) as well as the dimensionless quantities in eq. (7). Equation (1) is satisfied automatically, whereas, eq. (2), eq. (3) and eq. (4) constitutes these Ordinary differential equations:

$$f''' + ff'' - f'^2 + A^2 + M(A - f') + k_1 f' = 0 \quad \dots \quad (8)$$

$$\frac{1}{\text{Pr}} \left[ (1 + R_d \{1 + (\theta_w - 1) \theta\}^3) \theta' \right] + f \theta' + N_b \theta' \phi' + N_t \theta'^2 + E_c f'^2 + ME d(A - f')^2 = 0 \dots (9)$$

$$\phi'' + Lef \phi' + \frac{N_t}{N_b} \theta'' + Nd = 0 \quad \dots \quad (10).$$

Furthermore, when  $A = 0$ , the exact solution of Eq. (5) may be determined by using

$$f = (1 - e^{-\sqrt{1+M}\eta}) / \sqrt{1+M}, \text{ where } T \text{ is the temperature, } C \text{ is the concentration of nanoparticles, } C_f \text{ is the fluid's specific heat, and } D_B \text{ and } D_T \text{ are the Brownian motion and thermophoretic diffusion coefficients, respectively}$$

Where prime represents differentiation with respect to the function  $\eta$ ,  $M = \frac{\sigma_e B_0^2}{a \rho_f}$  is the

magnetic parameter,  $A = \frac{b}{a}$  is the ratio of the rates of free stream velocity to the velocity of the stretching sheet.

Eqs. (8)– (10) are subject to the following boundary conditions

$$\begin{aligned} f(0) = 0, f'(\infty) = A, f'(0) = 1, \\ \theta'(0) = -B[1 - \theta(0)], \\ \theta(\infty) = 0, \varphi(0) = 1, \varphi(\infty) = 0 \end{aligned} \quad (11)$$

Some of the parameters involved in Eqs. (8)– (10) are defined as follows

$$\begin{aligned} Le = \frac{v_f}{D_B}, Nb = \frac{\tau D_B (C_w - C_\infty)}{v_f}, \\ Nt = \frac{\tau D_B (T_f - T_\infty)}{v_f T_\infty}, Bi = \frac{h(v_f/a)^{1/2}}{k}, \\ Ec = \frac{U_w^2(x)}{C_n(T_w - T_\infty)}, \\ \varphi(\eta) = C - C_\infty / C_w - C_\infty, \\ k_1 = \frac{ax\mu_e}{k}, Nd = \frac{T_w D_{CT}}{D_B C_w}. \end{aligned}$$

The Lewis number is Le, the Brownian motion parameter is Nb, the thermophoresis parameter is Nt, the Biot number is Bi, impermeability of the surface  $k_1$ , Dufour diffusivity Nd, and Eckert number is Ec. The Nusselt number, Nu, and the Sherwood number, Sh, are the quantities of practical interest. As previously stated, the x-coordinate does not fit into the temperature equation. As a result, we try for the most local similarity solutions conceivable. The wall heat flux and wall mass flux, denoted by  $q_w$  and  $q_m$ , are supplied as follows:

$$\begin{aligned} q_w = -k \left( \frac{\partial T}{\partial y} \right)_{y=0} + (q_r)_w = \\ -k(T_w - T_\infty)(a/v_f)^{1/2} [1 + N\theta_c^3] \theta'(0), \\ q_m = -D_B \left( \frac{\partial C}{\partial y} \right)_{y=0} = \\ -D_B(C_w - C_\infty)(a/v_f)^{1/2} \varphi'(0) \dots \quad (12). \end{aligned}$$

By introducing the Nusselt number  $Nu_x = xq_w/k(T_f - T_\infty)$  and local Sherwood number  $Sh = xq_m/D_B(C_w - C_\infty)$  and the relation becomes

$$\begin{aligned} \frac{Nu_x}{\sqrt{Re_x}} = -[1 + R_d \theta_w^3] \theta'(0) = Nur, \\ \frac{Sh}{\sqrt{Re_x}} - \varphi'(0) = Shr \dots \quad (13). \end{aligned}$$

Such that  $Re_x = u_w(x)/\nu$  is the local Reynolds number of the nanofluid in this research.

## II. RESULT AND DISCUSSION:

Figs. 2 –13 are prepared to explore the characteristics of non-dimensional velocity, temperature and nanoparticles concentration as well as Nusselt number and Sherwood number for distinct values of emerging parameters like impermeability parameter  $k_1$ , Dufour diffusivity parameter Nd, Radiation parameter  $R_d$ , Biot number Bi, magnetic parameter M, heat generation/absorption parameter  $\lambda$ . Brownian motion parameter Nb, Prandtl number Pr, thermophoresis parameter Nt, Eckert number Ec, Lewis number Le, chemical reaction parameter  $\gamma$ . Were as, Table1 and Table2 are constructed in order to compare the present results with with the previous published results for validation.

**Table1:**

Results validation for the Nusselt number (-  $\theta'(0)$ ) when  $Rd = 0$ ,  $Pr = 10$ ,  $k_1 = 0$ ,  $Le = 10$ ,  $Nd = 0$  and  $Nt = 0.1$ .

Present results	Ghasemi et al. (31)
0.9528	0.9528
0.5060	0.5057
0.2529	0.2527
0.1200	0.1196
0.0548	0.0546

**Table 2:**

Results validation for the Nusselt number(- $\varphi'(0)$ ) when  $Rd = 0$ ,  $Pr = 10$ ,  $k_1 = 0$ ,  $Le = 10$ ,  $Nd = 0$  and  $Nt = 0.1$ .

Present results	Ghasemi et al. (31)
2.1298	2.1295
2.2749	2.2744
2.5288	2.5288
2.7957	2.7955
3.0354	3.0353

Figure2 analyzed the influence of Radiation parameter ( $R_d$ ) alongside the impermeability parameter ( $k_1$ ) on the distribution of momentum profile. (a). ( $k_1 < 0$ ) and (b). ( $k_1 > 0$ ) Increment in the radiation parameter increases the momentum distribution irrespective of increase or decrease in the impermeability parameter. On fig3. an effect of radiation parameter is depicted on the temperature distribution, in which increase in the radiation parameter enhances the temperature distribution of the system either with positive or negative impermeability parameter. (a).  $k_1 < 0$  and (b).  $k_1 > 0$ .

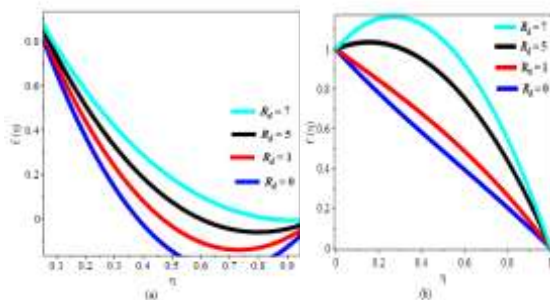


Figure2. effects of radiation parameter ( $R_d$ ) on momentum (a)  $k_1 < 0$  (b)  $k_1 > 0$ .

Fig.4 provide highlight on the distribution of radiation parameter ( $R_d$ ) towards dimensionless concentration alongside the impermeability of the surface, (a).  $k_1 < 0$  (b).  $k_1 > 0$ . Increase in the radiation parameter increases the concentration of the system.

Further observations from fig.5 shows the simultaneous effects of Magnetic parameter ( $M$ ) and impermeability of the surface over the temperature distribution, (a).  $k_1 < 0$  and (b).  $k_1 > 0$ . In this case, for (a). increase in the values of magnetic parameter ( $M$ ) implies decrease in the temperature profile whereas, on the other hand, increase in the values of magnetic parameter brings about increment in the temperature profile as in the case of (b).

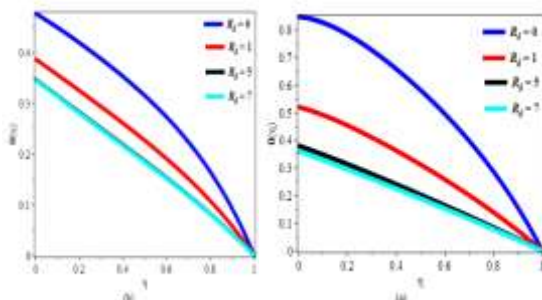


Figure3. effects of radiation parameter ( $R_d$ ) on temperature (a)  $k_1 < 0$  (b)  $k_1 > 0$ .

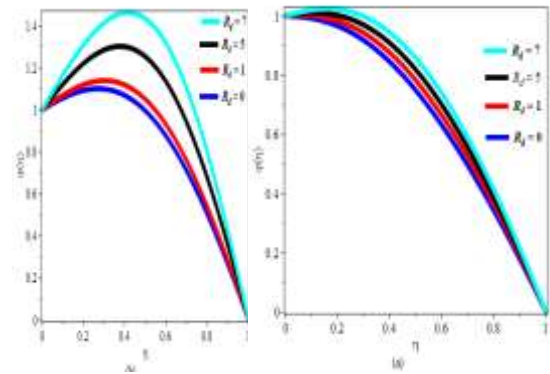


Figure4. effects of radiation parameter ( $R_d$ ) on concentration (a)  $k_1 < 0$  (b)  $k_1 > 0$ .

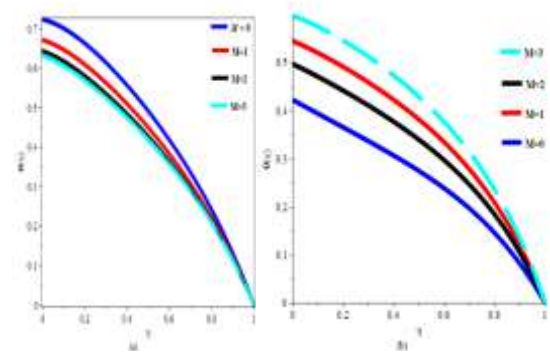


Figure5. effects of Magnetic parameter ( $M$ ) on temperature (a)  $k_1 < 0$  (b)  $k_1 > 0$ .

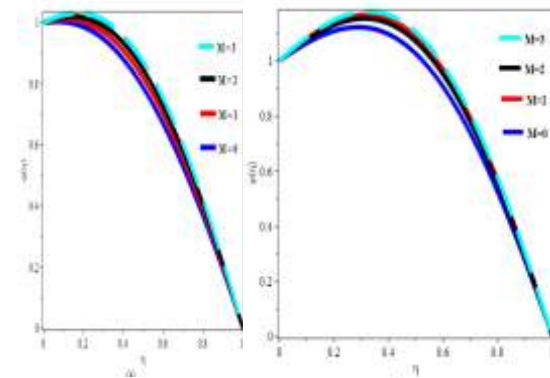


Figure6. effects of Magnetic parameter ( $M$ ) on concentration (a)  $k_1 < 0$  (b)  $k_1 > 0$ .



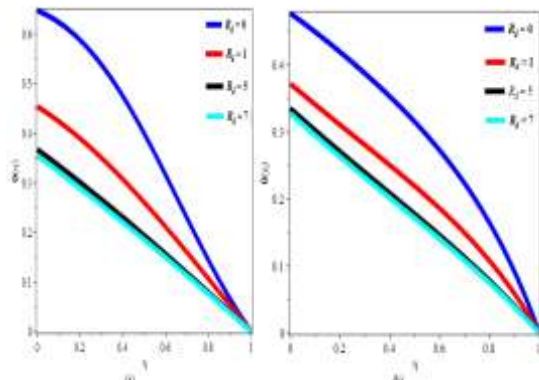


Figure7. effects of radiation parameter ( $R_d$ ) on temperature (a)  $Nd < 0$  (b)  $Nd > 0$ .

The variation of the dimensionless concentration with dual effects of magnetic parameter ( $M$ ) and impermeability is shown in Fig. 6 (a).  $k_1 < 0$  (b).  $k_1 > 0$ , for different values of magnetic parameter. In the absence of magnetic field, the dimensionless concentration at the surface is found to be higher and decreases with increasing magnetic field. It is important to note that irrespective of either the positivity or negativity of the impermeability of the surface, increase in the magnetic field intensity increases the concentration of the system. Furthermore, the dual effects of radiation parameter and Dufour diffusivity on the dimensionless temperature for different values of radiation parameter are depicted in Fig. 7 (a).  $Nd < 0$  and (b).  $Nd > 0$ . It can be seen that, the dimensionless temperature at the surface is higher for larger values of radiation parameter in all the cases for both (a) and (b).

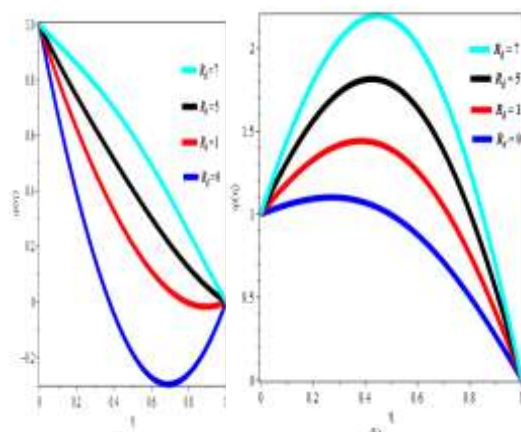


Figure8. effects of radiation parameter ( $R_d$ ) on concentration (a)  $Nd < 0$  (b)  $Nd > 0$ .

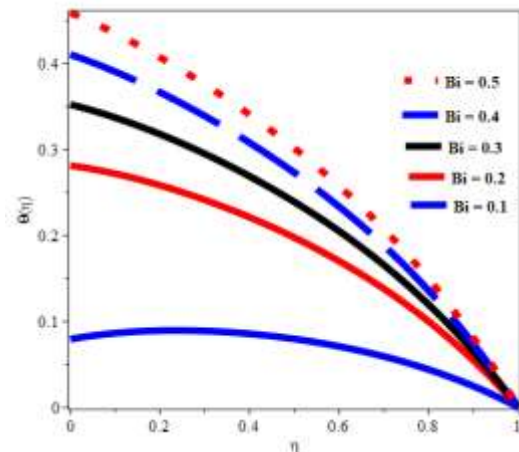


Figure9. Effects on Biot number ( $Bi$ ) on temperature

Fig. 8, depicted the variation in dimensionless rescaled nanoparticle volume fraction with different values of radiation parameter along with the Dufour diffusivity ( $Nd$ ). (a)  $Nd < 0$  and (b)  $Nd > 0$ . In both cases the concentration boundary layer thickness increases with increase of radiation parameter irrespective of positivity or negativity of the Dufour diffusivity. The effects of Biot number on the dimensionless temperature is shown in Fig. 9. It is clear that the temperature profile increases with increasing values of the Biot number ( $Bi$ ). The variation of momentum profile with different values of impermeability parameters is shown in Fig. 10 for stretching and shrinking sheets. It is clear from Fig. 10 that the momentum profile is accelerated with the increase in the values for impermeability of the surface. On the other hand, the influences of heat generation/absorption parameter over the Nusselt number is depicted on fig.11, in this case, it is observed that with heat absorption ( $\lambda < 0$ ), increase in the values of the parameter decreases the Nusselt number, whereas, with heat generation ( $\lambda > 0$ ), increase in the values of the parameter increases the Nusselt number. The variation of Sherwood number with different values of heat generation/absorption parameter is displayed on fig.12, in which it is clearly visible that increase in the heat generation/absorption parameter produces an increment in the values of Sherwood number. The simultaneous influence of radiation parameter as well as the Dufour diffusivity parameter on the Nusselt number profile is depicted on fig.13, dual increment of the parameters produces an increment in the Nusselt number profile.

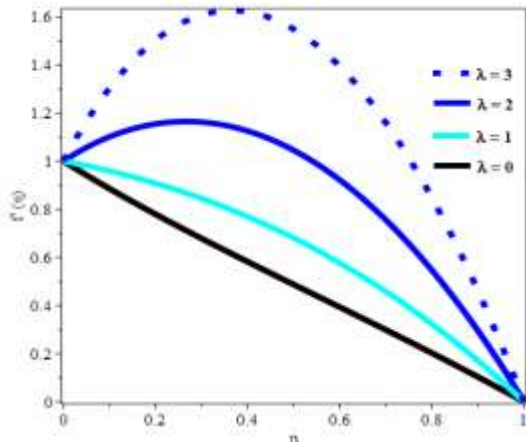


Figure 10. effects of heat generation/absorption ( $\lambda$ ) on Momentum

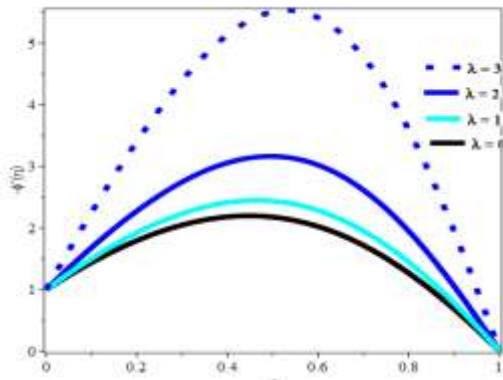


Figure 12. effects of heat generation ( $\lambda$ ) on Sherwood number profile

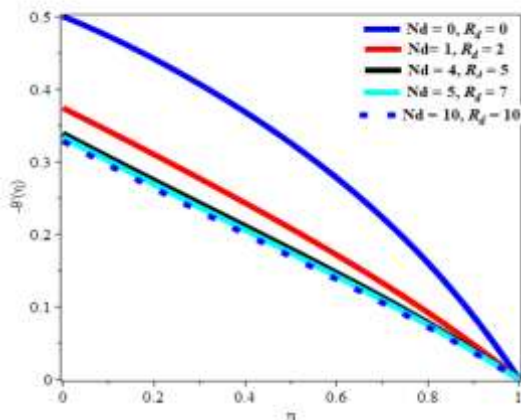


Figure 13. Simultaneous effects of Radiation parameter ( $R_d$ ) and Dofour diffusivity ( $N_d$ ) on the Nusselt number profile.

### III. CONCLUSION

The dual impacts of Dufour diffusivity along with impermeability of the surface towards a

convective Magnetohydrodynamic (MHD) stagnation point flow over a stretching sheet is addressed. The ODEs are resolved by employing R–K procedure along with Shooting technique. The influence of embedded variables on the distribution of velocity, temperature, concentration as well as Nusselt number and Sherwood number are illustrated graphically and tables. The key findings are stated below:

- Temperature is reduced while concentration and Nusselt number are increased with larger  $N_d$  and  $M$ .
- Depreciation is detected for Nusselt number and temperature to the enriched values of  $k_1$ .
- Strengthening of Biot number causes intensification in the temperature of the fluid.
- Both Nusselt number and Sherwood number enlarged with the escalation of heat generation/absorption parameter
- The heat transfer rate declaims for the growth in non-linear radiation parameter while reverse is the case for Nusselt number, velocity and concentration.

### Creditauthorshipcontribution statement

Abubakar Assidiq Hussaini:

Writing of the original draft, Conceptualization, Software work, as well as Methodology.

Adamu Abdulkadir Tata and Ja'afar Aliyu:

Review of the original writing, Validation, Data curation, along with editing Visualization.

### Declaration of competing interest:

The authors have no any Conflict of interest.

### References

- [1]. Zainal, N. A.;Nazar, R.; Naganthran,K;and Pop, I., (2021), "MHD flow and heat transfer of Hybrid nanofluid over a permeable moving surface in the presence of thermal radiation," Int. J. Numer Methods Heat Fluid Flow. 31 (3). 858- 879
- [2]. Hussaini, Abubakar Assidiq; and Abdulkadir, Adamu Tata, (2022), "Physical effects of heat generation/ absorption on MHD nanofluid flow over a stretching surface,"Int. J. Adv. Eng. and Mang. (IJAEM). 4 (6) 1464-1478.DOI: 10.35629/5252-040614641478.
- [3]. Nield, D.A; and Kuznetsov, A.V. (2009). "The Cheng-Minkowycz problem for natural convective boundary layer flow in a porous medium saturated by a nanofluid." Int. J. Heat Mass Transfer 52, 5792–5795.

- [4]. Shang, J.S. (2001). "Recent research in magneto-aerodynamics." *Prog. Aero. Sci.* 37, 1–20.
- [5]. Shu, C. (2012). "Differential Quadrature and its Application in Engineering." Springer.
- [6]. Subhas M.; Abel; and Nandeppanavar, M.M. (2007). "Effects of thermal radiation and non-uniform heat source on MHD flow of viscoelastic fluid and heat transfer over a stretching sheet." *Int. J. Appl. Mech. Eng.* 12 (4), 903–918.
- [7]. Talebizadeh, P., Moghimi, M.A., Kimiaefar, A. & Ameri, M. (2011). "Numerical and analytical solution for natural convection flow with thermal radiation and mass transfer past a moving vertical porous plate by DQM and HAM," *Int. J. Comput. Methods* 8, 611–631.
- [8]. Hussaini, A. A., Madaki, A.G. and Kwami A.M. (2021). "Modified Mathematical Model on the Study of Convective MHD Nanofluid flow with Heat Generation/Absorption." *Int. J. Engineering research and technology*, 10 (09), 155- 163.
- [9]. Hussaini, A. A., Madaki, A. G., Alaramma, S.K. and A. Barde, (2022). "Numerical Study on the Influence of Thermophores and Magnetic Field on the Boundary Layer Flow Over a Moving Surface in a Nanofluid." *Int. J. Scientific Research and Modern Technology*. 2 (1), 4- 9.
- [10]. Hussaini, A. A.; Abdullahi, Isah; Abdulkadir, Adamu Tata; and Musa, Ali, (2022), "Numerical Approach to Determine the Simultaneous Influence of Thermal Radiation and Chemical Reaction Over MHD Stagnation-Point Flow of Sisko Nanofluid." *Iconic Res. and Eng. J. (IRE)*. 5 (9) 2456-8880
- [11]. Ijaz, M.; Ayub, M.; Malik, M.Y.; Khan, H., Alderremy, A.A.; and Aly, S., (2020). "Entropy analysis in nonlinearly convective flow of the Sisko model in the presence of Joule heating and activation energy: The Buongiorno model," *Phys. Scripta* 95 (2) 025402
- [12]. Pal, Dulal; and Mandal Gopinath (2020). "Magnetohydrodynamic stagnation-point flow of Sisko nanofluid over a stretching sheet with suction," *Propuls. Power Res.* 9(4): 151- 158.
- [13]. Zainal, N.A.; Nazar, R.; Naganthran, K.; and Pop, I. (2021). "Unsteady EMHD stagnation point flow over a stretching/ shrinking sheet in a hybrid  $Al_2O_3$ -Cu/ $H_2O$  nanofluid." *Int. Comm. Heat Mass Transfer*. 123105236.
- [14]. Hussaini, Abubakar Assidiq; Madaki, Abdullahi Gamsha; Kabiru, Sanusi Alaramma; Barde, Aminu; and Abdullahi, Isah, (2022). "Numerical Approach for Convective Magnetohydrodynamic (Mhd) Nanofluid Flow with Impermeable Stretching Surface." *The Sciencetech.* 3(1), 1- 16.
- [15]. Said Z.; and Sohail M.A., (2022). "Introduction to Hybrid nanofluids (a volume in micro and nanotechnologies book)." 1- 32, <http://doi.org/10.1016/B978-0-323-858336-6.00001-6>.
- [16]. Sadaf Masood; Muhammad Farooq; and Aisha Anjum, (2021), "Influence of heat generation/ absorption and stagnation point on polystyrene- $TiO_2/H_2O$  hybrid nanofluid flow." *J. Sci. research*, 11: 22381 | <https://doi.org/10.1038/s41598-021-01747-9>
- [17]. Khashi'ie, N.S.; Arifin, N.M.; Pop, I.; and Nazar, R. (2020), "Melting heat transfer in Hybrid nanofluid flow along a moving surface," *J. Therm. Anal. Calorim.* <https://doi.org/10.1007/s10973020-10238-4>.
- [18]. Suganya, S.; Muthamilselvan, M.; and Alhussain, Z.A., (2021). "Activation energy and Coriolis force on Cu- $TiO_2$ /water hybrid nanofluid flow in an existence of nonlinear radiation," *Appl. Nanosci.* 11 933.
- [19]. Bakar, S.A.; Arifin, N.M.; Khashi'ie, N.S. and Bachok N., (2021). "Hybrid Nanofluid Flow over a Permeable Shrinking Sheet Embedded in a Porous Medium with Radiation and Slip Impacts." *Mathematics* 9(8) 878
- [20]. Khashi'ie, N.S.; Waini, I.; Zainal, N.A. Hamzah, K. and Kasim, A.R.M., (2020), "Hybrid Nanofluid Flow Past a Shrinking Cylinder with Prescribed Surface Heat Flux." *Symmetry* 12(9) 1493.
- [21]. Waini, I.; Ishak, A.; and Pop I., (2020). "Hybrid nanofluid flow towards a stagnation point on a stretching/shrinking cylinder." *Sci. Rep.* 10 (1) 1–12.
- [22]. Sudarsana, Reddy P.; and Chamkha Ali J. (2016). "Soret and Dufour effects on MHD convective flow of  $Al_2O_3$ - water and  $TiO_2$ -water nanofluids past a stretching sheet in porous media with heat generation/absorption." *J. adv. Power Tech.* 1-13. <https://dx.doi.org/10.1016/j.appt.2016.04.005>.

- [23]. Mahabaleshwar, U.S.; Nagaraju, K.R.; Vinay, Kumar P.N.; Nadagoud, M.N. Bennacer, R; and Sheremet, M. A. (2019). "Effects of Dufour and Soret mechanisms on MHD mixed convective- radiative non- Newtonian liquid flow and heat transfer over a porous sheet." *Therm. Sci. & Eng. Prog.* <https://doi.org/10.1016/j.tsep.2019.100459>.
- [24]. Ali, Bagh; Hussain, Sajjad; Nie, Yufeng; Khadim, Ahmed Hussein; Habib, Danial, (2021). "Finite element investigation of Dufour and Soret impacts on MHD rotation flow of Oldroyd-B nanofluid over a stretching sheet with double diffusion Cattaneo Christov heat flux model." 377, 439- 452. <https://doi.org/10.1016/j.powtec.2020.09.008>.
- [25]. Shateyi, Stanford; Sydney, Sandile Motsa; and Sibanda, Precious, (2009). "The effects of Thermal Radiation, Hall Currents, Soret, and Dufour on MHD Flow by mixed convection over a vertical surface in porous Media." 627475. Doi://10.1155/2010/627475.
- [26]. Zhao, Jinhui; Zheng, Liancun; Zhang, Xinxin; and Liu, Fawang, (2016). "Convection heat and mass transfer of fractional MHD Maxwell fluid in a porous medium with Soret and Dufour effects." *Int. J. heat mass transfer.* 103, 203- 210. <https://dx.doi.org/10.1016/j.ijheatmasstransfer.2016.07.057>.
- [27]. Hayat, Tasawar; Nasir, Tehreem; Ijaz, Muhammad Khan; and Alsaedi, Ahmed, (2018). "Numerical investigation of MHD flow with Soret and Dufour effects." *J. Results in Phy.* 8 1017- 1022. <https://doi.org/10.1016/j.rinp.2018.01.006>.
- [28]. Poc, Pascal; Gutzeit, A. Vanessa; Ast, Julia; Lee, Joon; Jones, J. Ben; D'Este Elisa; Mathes, Bettina; Lehmann Martin; Hodson, J. David; Levitz, Joshua; and Broichhagen, Johannes, (2020). "Interrogating surface versus intracellular transmembrane receptor populations using cell- impermeable SNAP-tag substrate." *The Royal Soc. Chem.* <https://doi:10.1039/d0sc02794d>.
- [29]. Zhang, Bingliu; Tan, Hongbo; Shen, Weiguo; Xu, Gelong; Ma, Baoguo; and Ji, Xiaoli, (2018). "Nano- silica and silica fume modified cement mortar used as surface protection material to enhance the impermeability." *Cem. Con.* [comp.https://doi:10.1016/j.cemconcomp.2018.05.012](https://doi:10.1016/j.cemconcomp.2018.05.012).
- [30]. Patil, P.M; Roy, S; and Mominiat E. (2016). "Thermal diffusion and diffusion- thermo effects on mixed convection from an exponentially impermeable stretching surface." *Int. J. Heat Mass Trans.* 100, 482-489. <https://dx.doi.org/10.1016/j.ijheatmasstransfer.2016.04.054>.
- [31]. Ghasemi, S.E.; and Hatami, M. (2021). "Solar radiation effects on MHD stagnation point flow and heat transfer of a nanofluid over a stretching sheet." *Case Studies in Thermal Engineering* 25, 100898. <https://doi.org/10.1016/j.csite.2021.100898>.
- [32]. Mushtaq, Ammar; Mustafa, M.; Hayat T.; and Alsaedi A. (2014). "Nonlinear radiative heat transfer in the flow of nanofluid due to solar energy: A numerical study." *J. Taiwan inst. Chem. Eng.* 45 (4). 1176- 1183.
- [33]. Ghasemi, Seiyed E.; Hatami, M.; Jing, D.; and Ganji, D.D. (2016). "Nanoparticles effects on MHD fluid flow over a stretching sheet with solar radiation: A numerical study." *J. Molliq.* 890- 896. <https://doi.org/10.1016/j.molliq.2016.03.065>